A Very Rare Example of a Structurally Characterized 3′-GMP Metal Complex. NMR and Synthetic Assessment of Adducts Formed by Guanine Derivatives with [Pt(L^{tri})Cl]Cl Complexes with an *N,N′,N″* Tridentate Ligand (L^{tri}) Terminated by Imidazole Rings

Supporting Information

*Kokila Ranasinghe, Svetlana Pakhomova, Patricia A. Marzilli, and Luigi G. Marzilli**

Department of Chemistry, Louisiana State University, Baton Rouge, Louisiana 70803, United States

E-mail: lmarzil@lsu.edu

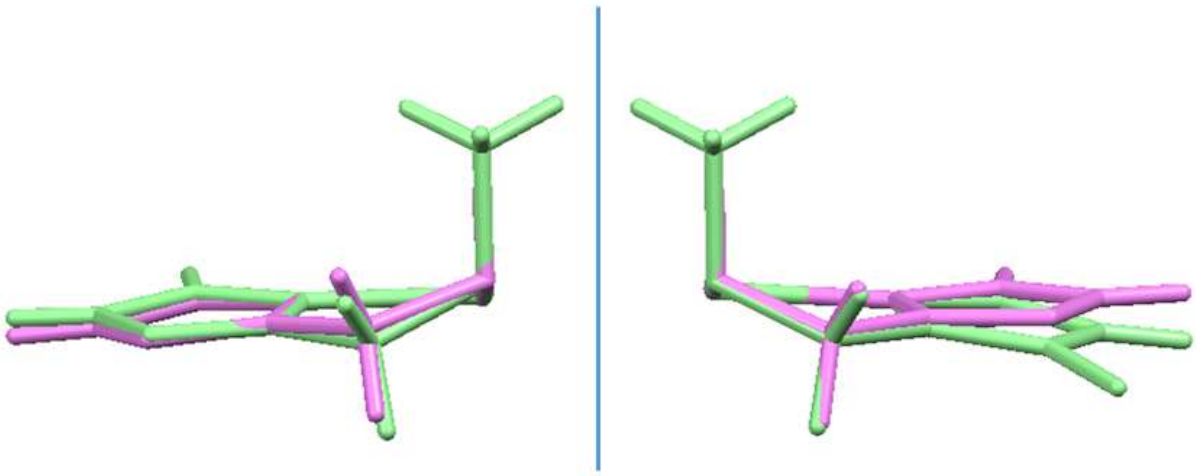

Figure S1. Tilting of the imidazolyl rings in the [Pt(*N*(R)1,1′-Me_2dma)Cl]BF_4 cations (overlay of **3b** (R = H, pink) and **4b** (R = Me, green) by superimposing the Pt, N2, and N3 atoms (*left*) and Pt, N2, and N1 atoms (*right*) viewed along the coordination plane. In order to display the tilting clearly, only parts of one chelate ring are shown in each half of the figure, and the N-Me group on each imidazolyl ring is hidden. The figure shows that the methylene groups are farther on the other side of the coordination plane from the NH or NMe group in the R = Me cation.

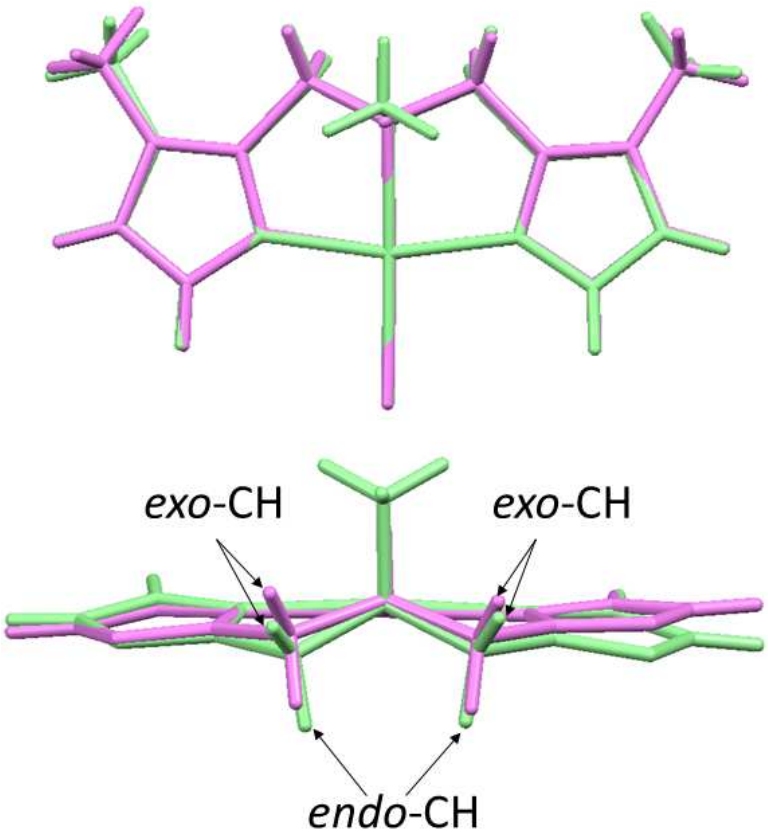

Figure S2. Overlay of the [Pt(*N*(R)1,1′-Me_2dma)Cl]BF_4 cations, **3b** (R = H, pink) and **4b** (R = Me, green) by superimposing the Pt, Cl, N1, N2, and N3 atoms, viewed from the top (*top*) and along the coordination plane (*bottom*), where the *endo*-CH and the *exo*-CH protons are designated. For clarity, the N-Me groups of the imidazolyl rings are hidden in the bottom structure.

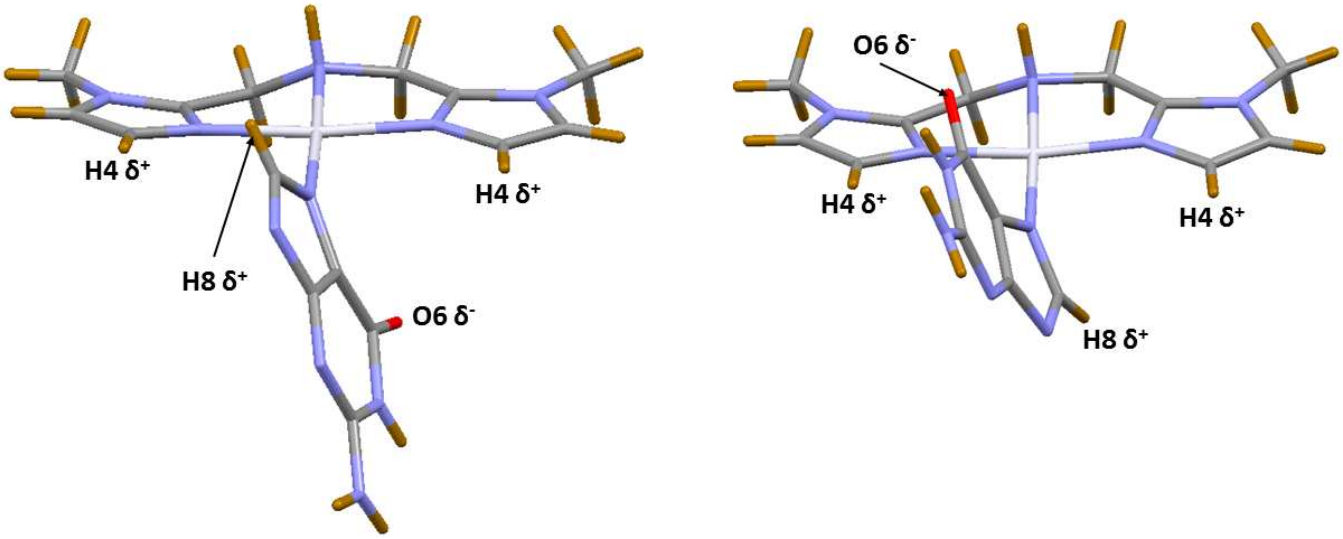

Figure S3. Models of the anti (*left*) and syn (*right*) rotamers of the Pt(*N*(H)1,1′-Me_2dma)(3′-GMP) adduct based on the molecular structure of **5** as described in the main text. The ribose and phosphate groups are hidden in order to display the models clearly.

Structural Features of the 3′-GMPH Ligand. Bond lengths and angles for the guanine rings are in the normal range found for nucleotides, e.g., 5′-GMP[1,2] and 3′-GMP.[3] The nucleotide conformation in **5** is anti, i.e., antiperiplanar (the C12─N6─C1′─O2 torsion angle around the N6─C1′ glycosidic bond is –164.9°).[4] The 5′-GMP has the anti conformation in all of the structurally characterized bis adducts of 5′-GMP[1,2,5,6] referred to in the main text discussion. The pucker of the ribose sugar group in **5** is C2′-*endo* (S pucker), as indicated by the 0.157 Å displacement in the C5′ direction of the C2′ atom from the plane defined by the C1′, C4′ and O2 atoms and by the pseudo-rotation phase angle P ~177°.[7] The ribose S puckering is retained in solution, as indicated by the H1′ and H2′ coupling constant of 4.8 Hz.[8,9] Most of the platinum **G** adducts described in the literature have ribose groups with similar S puckering.[2,9,10] Two of the terminal P─O bonds in **5** have lengths (P─O5, 1.492(9) Å, and P─O7, 1.471(8) Å) that are shorter than the P─O6 bond (1.574(9) Å), which is comparable in length to the P─OH bonds (1.536(1)–1.598(5) Å) of the bis complexes of 5′-GMP referenced above.[1,2,5,6] Thus, O6 in **5** is protonated, although an H atom at O6 is not visible in the electron density map.

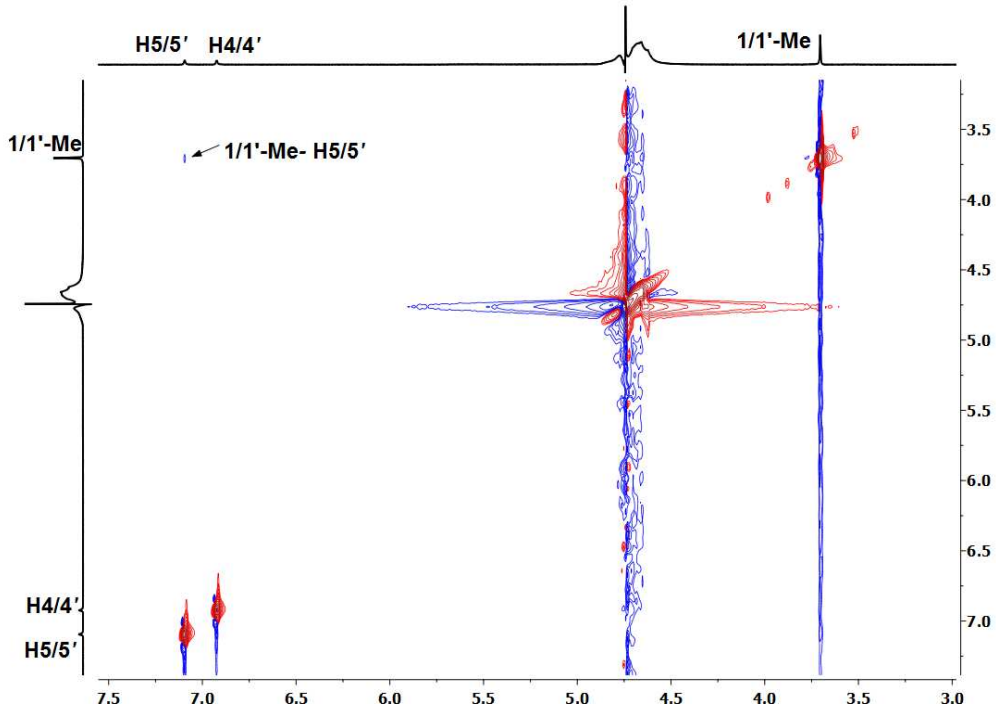

Figure S4. ^{1}H-^{1}H ROESY spectrum (selected region) of Pt(*N*(H)1,1′-Me$_2$dma)Cl]Cl (**3a**) (25 °C, D$_2$O, pH 6, shifts in ppm).

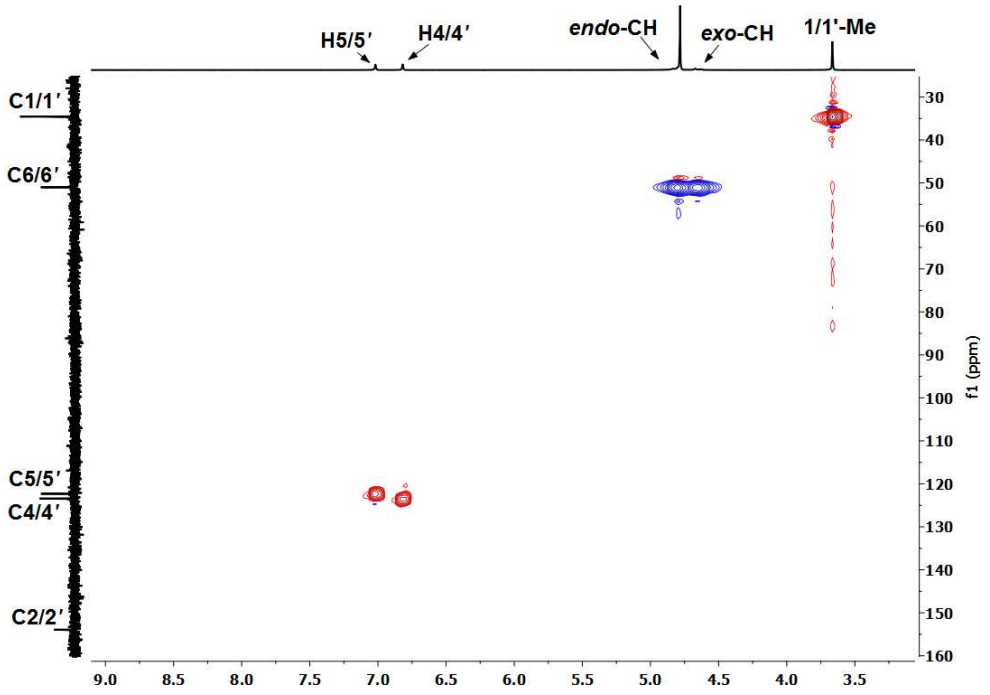

Figure S5. ^{1}H-^{13}C HSQC spectrum (aromatic region) of the [Pt(*N*(H)1,1′-Me$_2$dma)Cl]Cl (**3a**) complex (25 °C, D$_2$O, pH 6, shifts in ppm).

NMR Assignments for [Pt(*N*(Me)1,1′-Me$_2$dma)Cl]Cl (4a). As discussed in the main text, **4a** has downfield ^{1}H NMR signals for the H4/4′ and H5/5′ aromatic protons. In the ROESY spectrum in D_2O for **4a** (Figure S6), a strong NOE cross-peak from the 1/1′-Me signal at 3.78 ppm assigns the most downfield signal (7.19 ppm) to H5/5′. The other aromatic peak (7.05 ppm) can thus be assigned to H4/4′, an assignment supported by the NOE cross-peak to the H5/5′ signal and by the absence of any other cross-peak. By the reasoning used in the main text, the upfield and downfield methylene signals of **4a** were assigned to the *exo*-CH and *endo*-CH signals, respectively. Assignments of the ^{13}C NMR signals for **4a** were made through an HSQC experiment (Figure S7). ^{13}C NMR signals for the C4/4′, C5/5′, and C1/1′ were assigned with the aid of cross-peaks (in ppm) involving the H4/4′ (7.05−124.3), H5/5′ (7.20−122.6), Me-1/1′ (3.78−34.7) and N-Me (3.14−52.73) signals, respectively. Cross-peaks from the *endo*-CH and *exo*-CH signals assign the ^{13}C NMR signal at 61.95 ppm to C6/6′. The signal at 152.87 ppm, the only ^{13}C NMR signal with no HSQC cross-peak, is assigned to C2/2′.

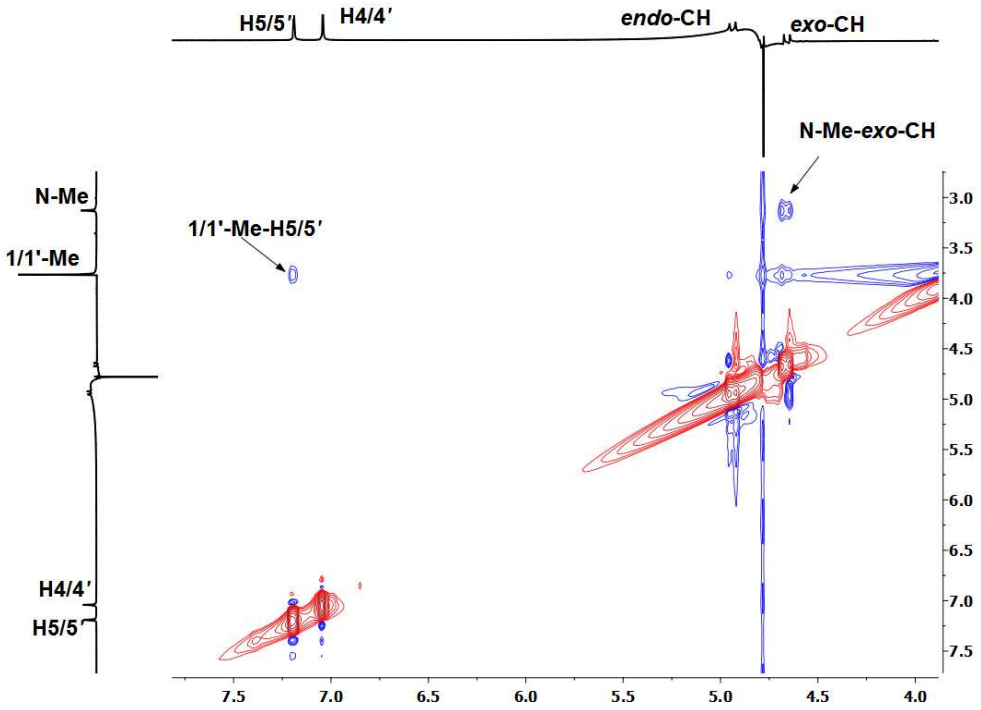

Figure S6. ^{1}H-^{1}H ROESY spectrum (selected region) of Pt(*N*(Me)1,1′-Me$_2$dma)Cl]Cl (**4a**) (25 °C, D_2O, pH 6, shifts in ppm).

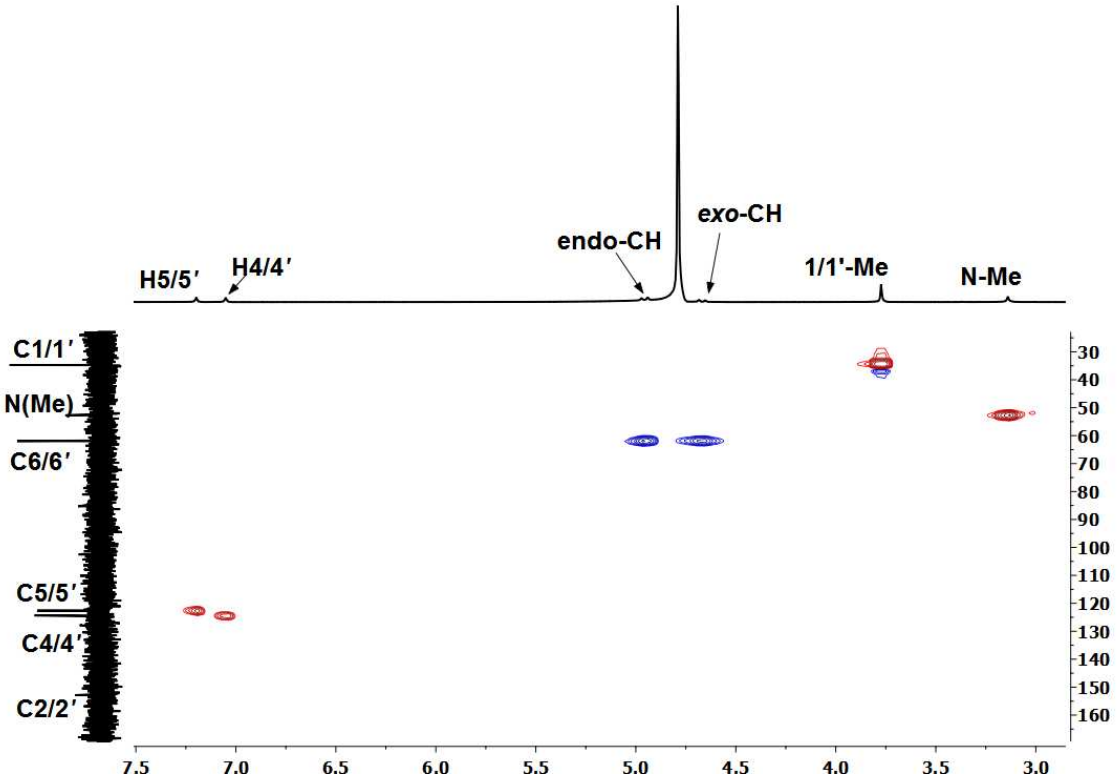

Figure S7. Selected region of a ^{1}H-^{13}C HSQC spectrum of [Pt(*N*(Me)1,1′-Me$_2$dma)Cl]Cl (**4a**) (25 °C, D$_2$O, pH 6, shifts in ppm).

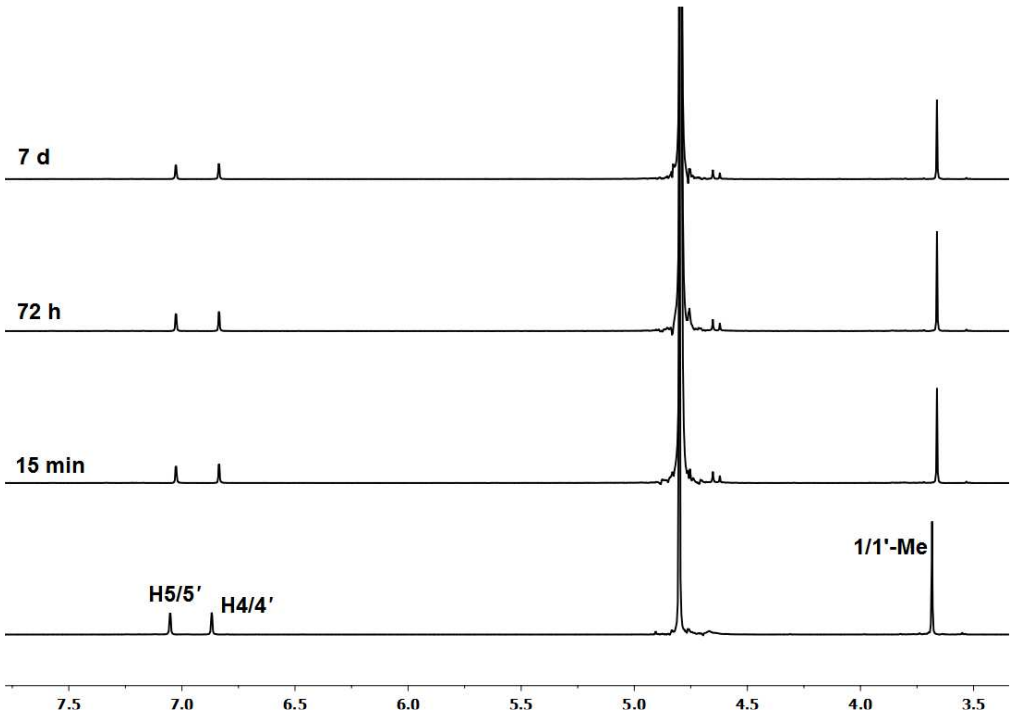

Figure S8. ^{1}H NMR spectra of a 10 mM solution (600 μL) of [Pt(*N*(H)1,1′-Me$_2$dma)Cl]Cl (**3a**) (25 °C, D$_2$O, shifts in ppm) at pH 7 before (*bottom*), and after adding 10 μL of concentrated HCl (final [H$^+$] = 0.2 M) at 15 min, 72 h and 7 d.

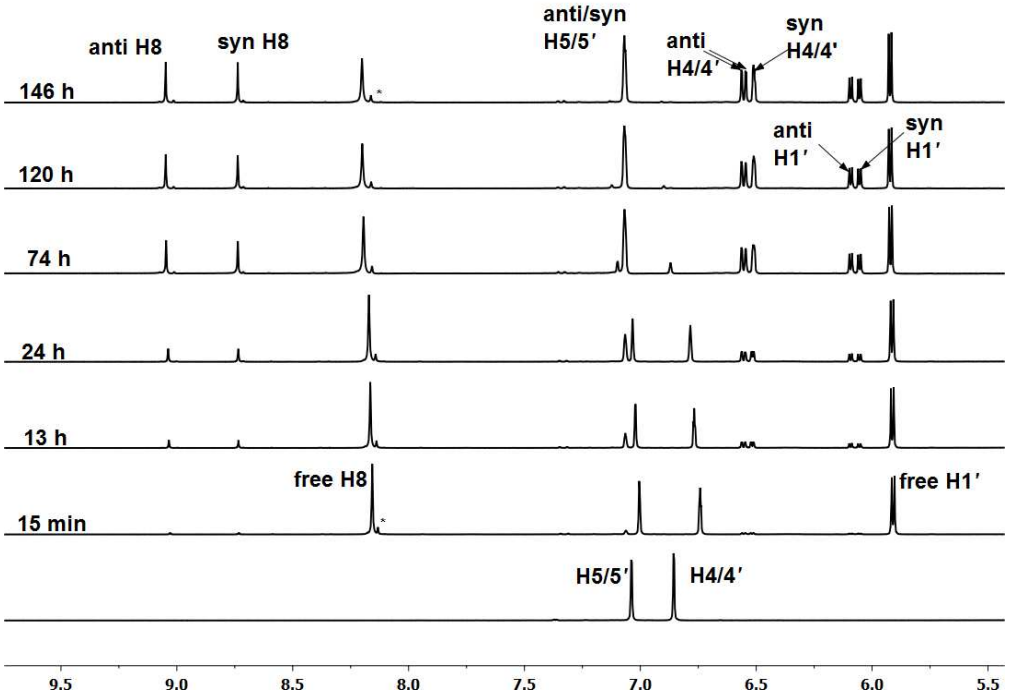

Figure S9. Aromatic and H1′ region of the ^{1}H NMR spectra of [Pt(*N*(H)1,1′-Me$_2$dma)Cl]$^{+}$ (10 mM, *bottom*) and of the reaction mixture with 5′-GTP (1:2.5 molar ratio, 25 °C, D_2O, pH 4.0, shifts in ppm). Peaks labeled as * are from 5′-GDP present as an impurity.

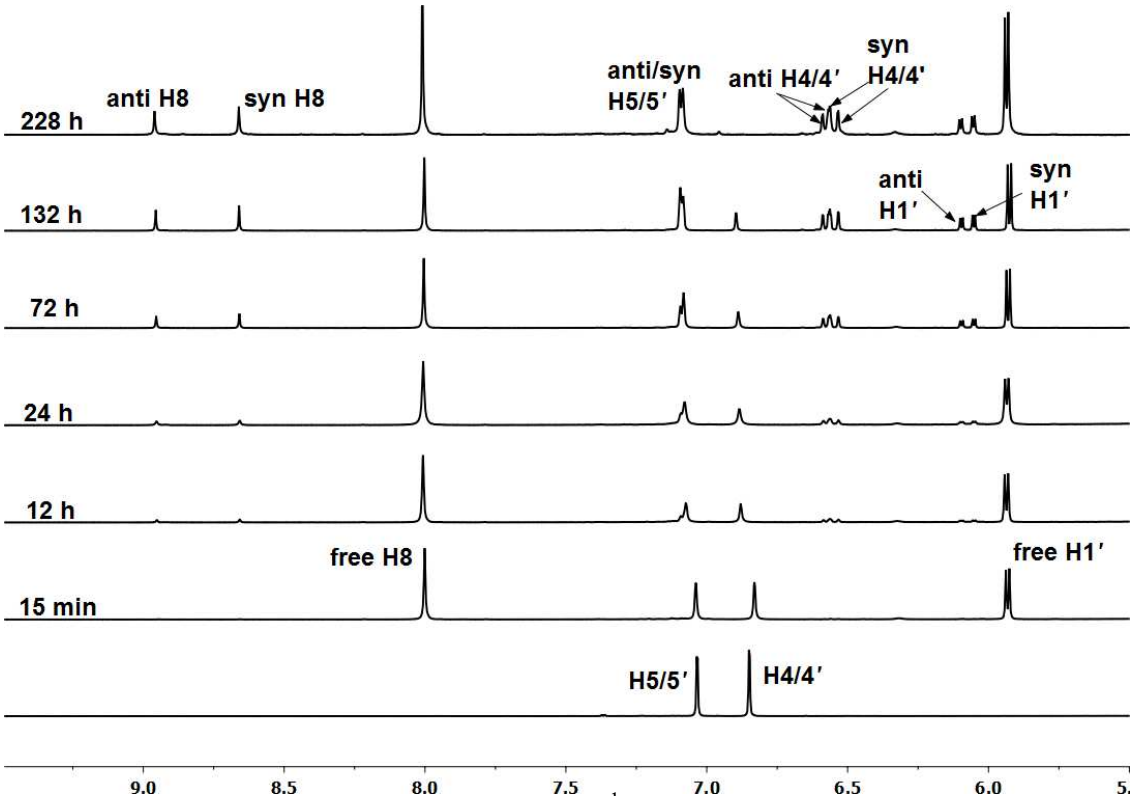

Figure S10. Aromatic and H1′ region of the ^{1}H NMR spectra of [Pt(*N*(H)1,1′-Me$_2$dma)Cl]$^{+}$ (10 mM, *bottom*) and of the reaction mixture with 3′-GMP (1:2.5 molar ratio, 25 °C, D_2O, pH 4.0, shifts in ppm).

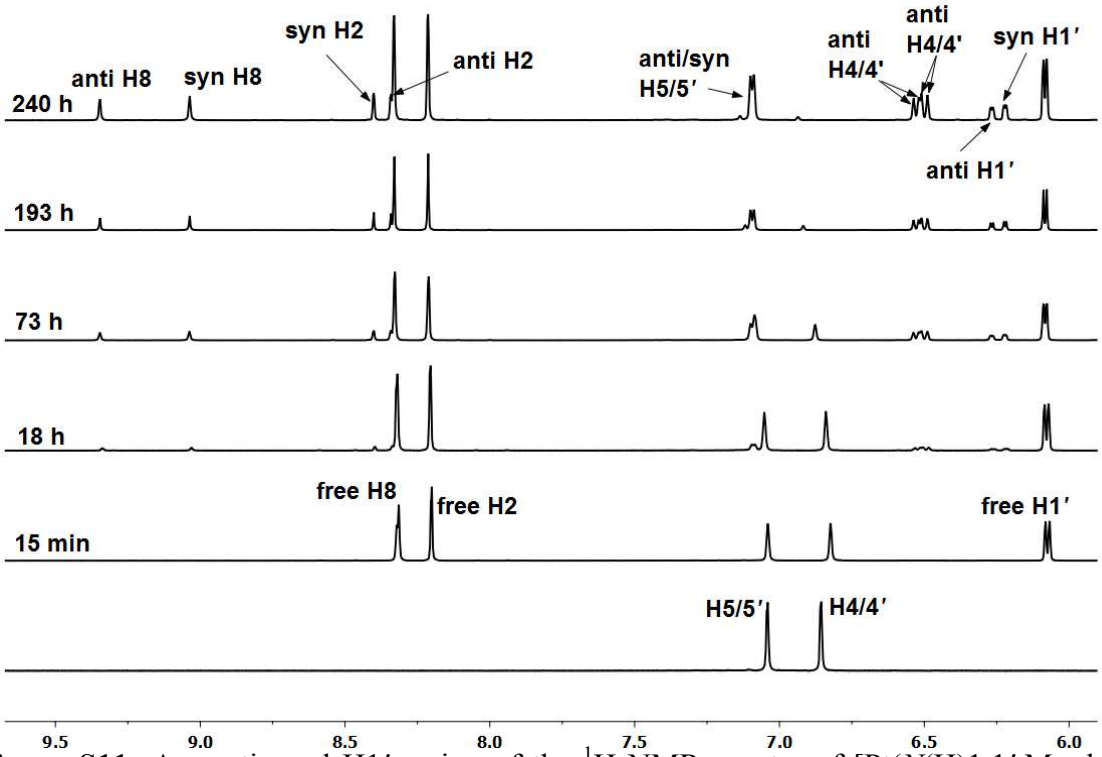

Figure S11. Aromatic and H1′ region of the ^{1}H NMR spectra of [Pt(*N*(H)1,1′-Me$_2$dma)Cl]$^+$ (10 mM, *bottom*) and of the reaction mixture with Ino (1:2.5 molar ratio, 25 °C, D_2O, pH 4.0, shifts in ppm).

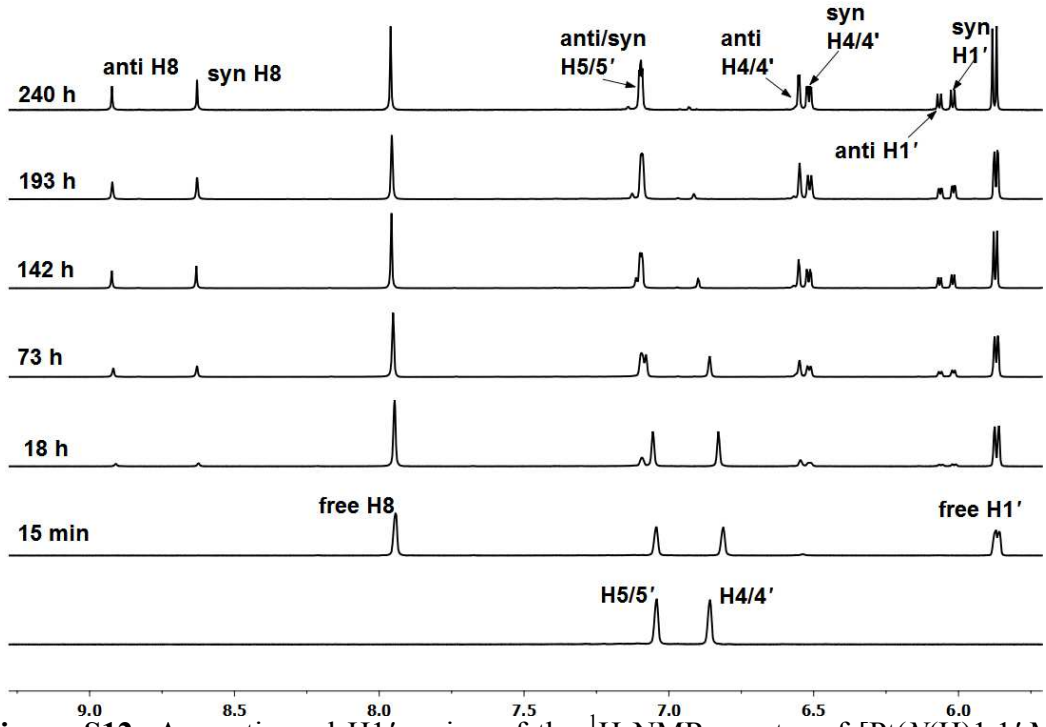

Figure S12. Aromatic and H1′ region of the ^{1}H NMR spectra of [Pt(*N*(H)1,1′-Me$_2$dma)Cl]$^+$ (10 mM, *bottom*) and of the reaction mixture with 1-MeGuo (1:2.5 molar ratio, 25 °C, D_2O, pH 4.0, shifts in ppm).

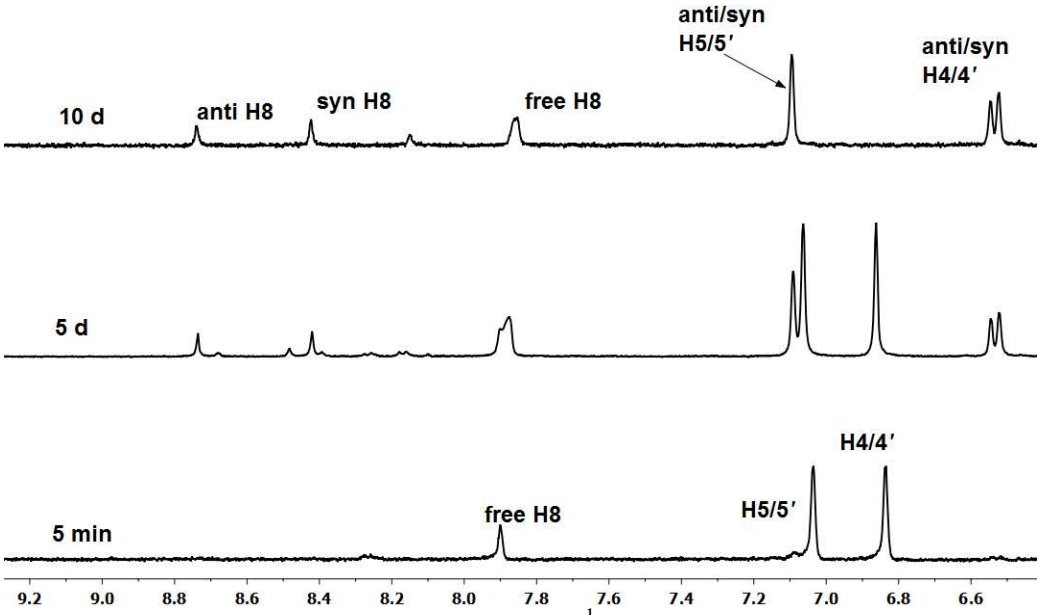

Figure S13. Aromatic and H1′ region of the ^{1}H NMR spectra of [Pt(*N*(H)1,1′-Me$_2$dma)Cl]$^{+}$ (10 mM, *bottom*) and of the reaction mixture with 9-EtG (1:2.5 molar ratio, 25 °C, D_2O, pH 4.0, shifts in ppm). Note that 9-EtG is only partially soluble in D_2O.

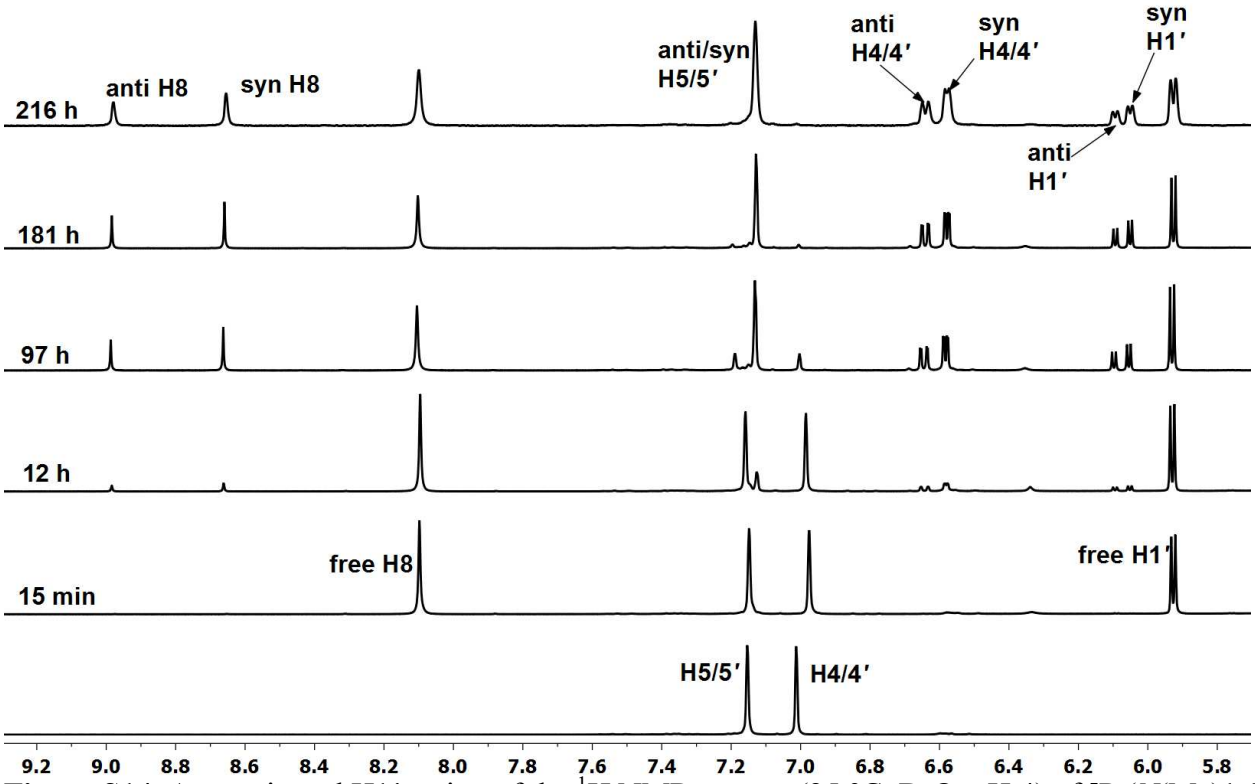

Figure S14. Aromatic and H1′ region of the ^{1}H NMR spectra (25 °C, D_2O, pH 4) of [Pt(*N*(Me)1,1′-Me$_2$dma)Cl]$^{+}$(10 mM, bottom) and of the reaction mixture forming Pt(*N*(Me)1,1′-Me$_2$dma)(5′-GMP) 15 min, 12 h, 97 h, 181 h and 216 h after adding 2.5 molar equiv of 5′-GMP (shifts in ppm).

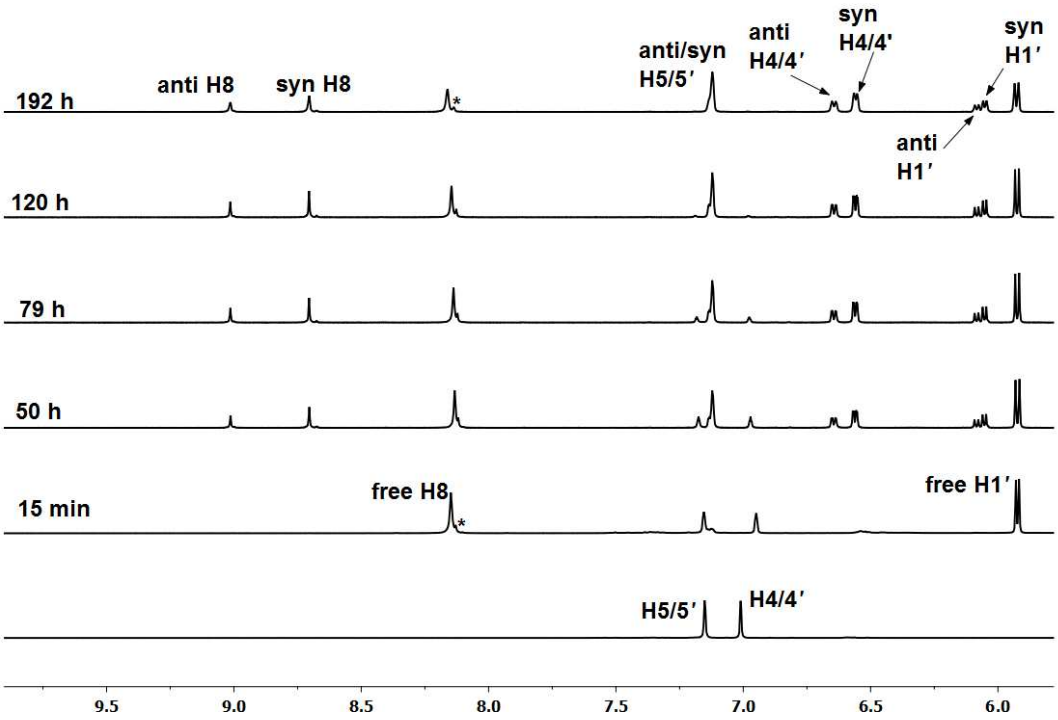

Figure S15. Aromatic and H1′ region of the ^{1}H NMR spectra of [Pt(*N*(Me)1,1′-Me$_2$dma)Cl]$^{+}$ (10 mM, *bottom*) and of the reaction mixture with 5′-GTP (1:2.5 molar ratio, 25 °C, D_2O, pH 4.0, shifts in ppm). Peaks labeled as * are from 5′-GDP present as an impurity.

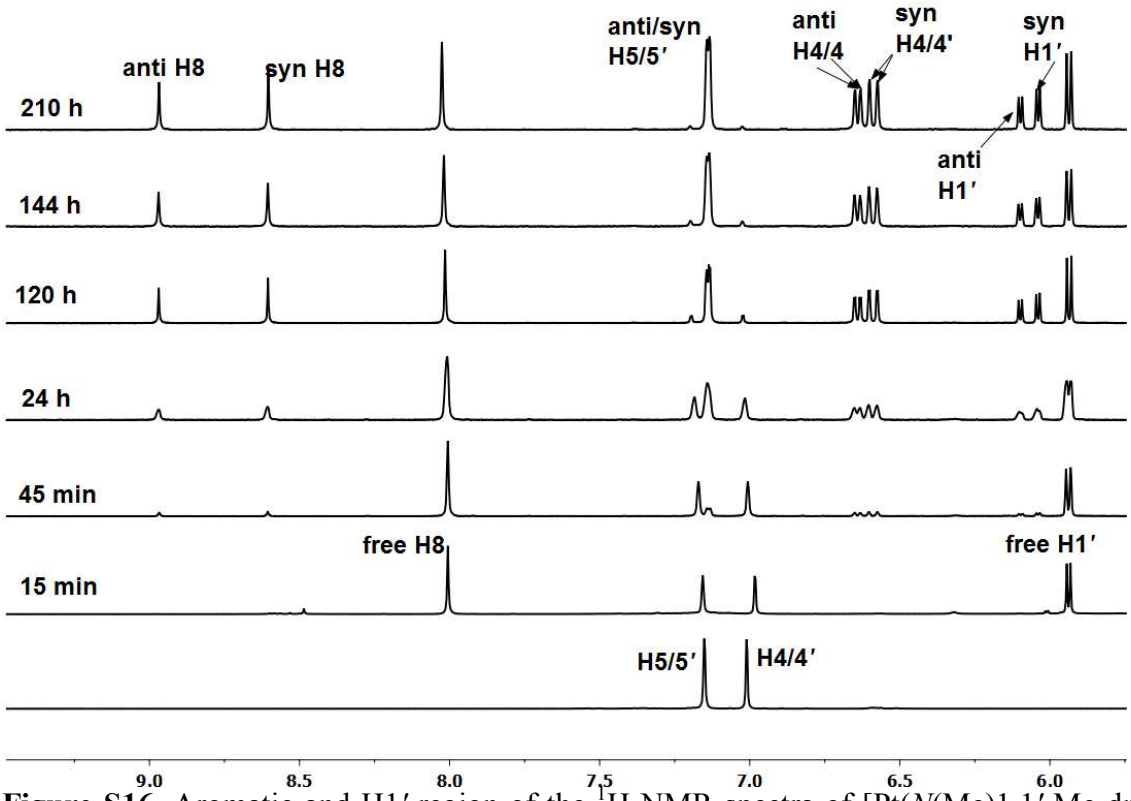

Figure S16. Aromatic and H1′ region of the ^{1}H NMR spectra of [Pt(*N*(Me)1,1′-Me$_2$dma)Cl]$^{+}$ (10 mM, *bottom*) and of the reaction mixture with 3′-GMP (1:2.5 molar ratio, 25 °C, D_2O, pH 4.0, shifts in ppm).

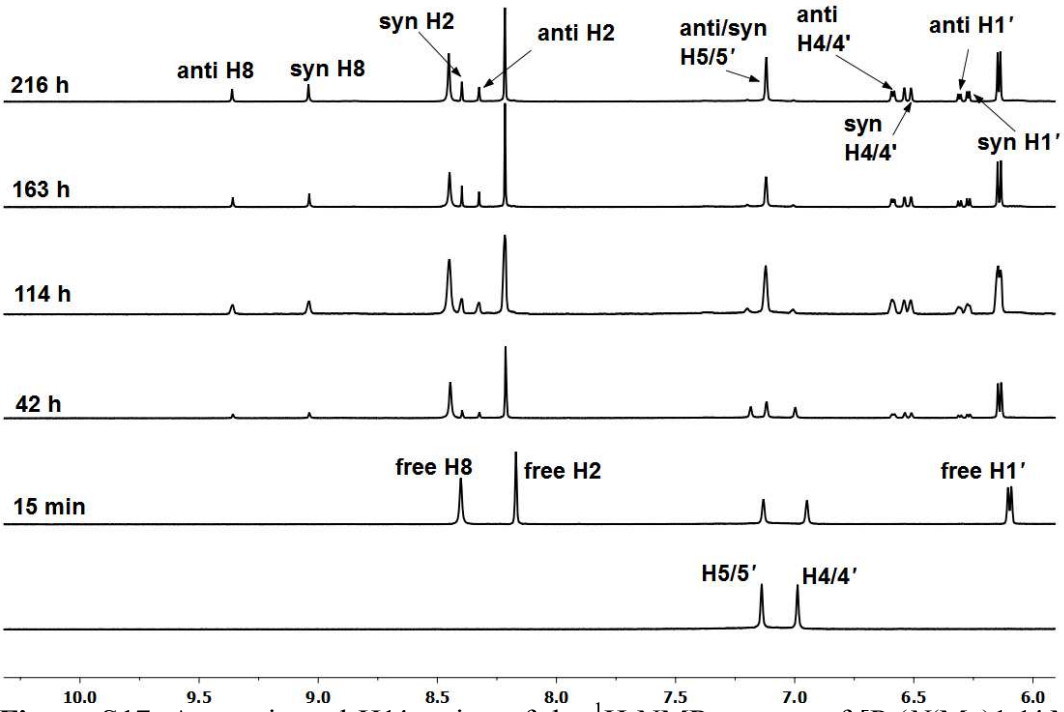

Figure S17. Aromatic and H1′ region of the ^{1}H NMR spectra of [Pt(*N*(Me)1,1′-Me$_2$dma)Cl]$^{+}$ (10 mM, *bottom*) and of the reaction mixture with 5′-IMP (1:2.5 molar ratio, 25 °C, D_2O, pH 4.0, shifts in ppm).

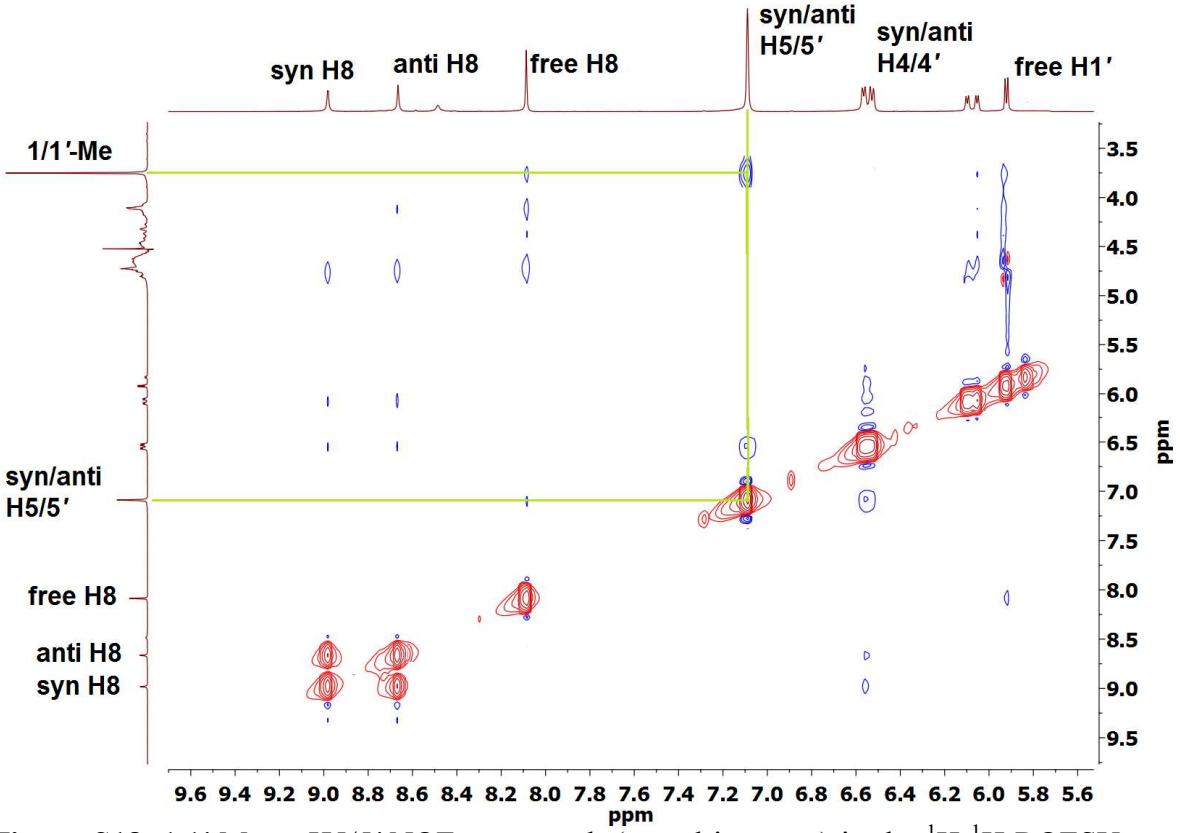

Figure S18. 1,1′-Me-to-H5/5′ NOE cross-peak (traced in green) in the ^{1}H-^{1}H ROESY spectrum of the Pt(*N*(H)1,1′-Me$_2$dma)(5′-GMP) adduct (25 °C, D_2O, pH 4, shifts in ppm).

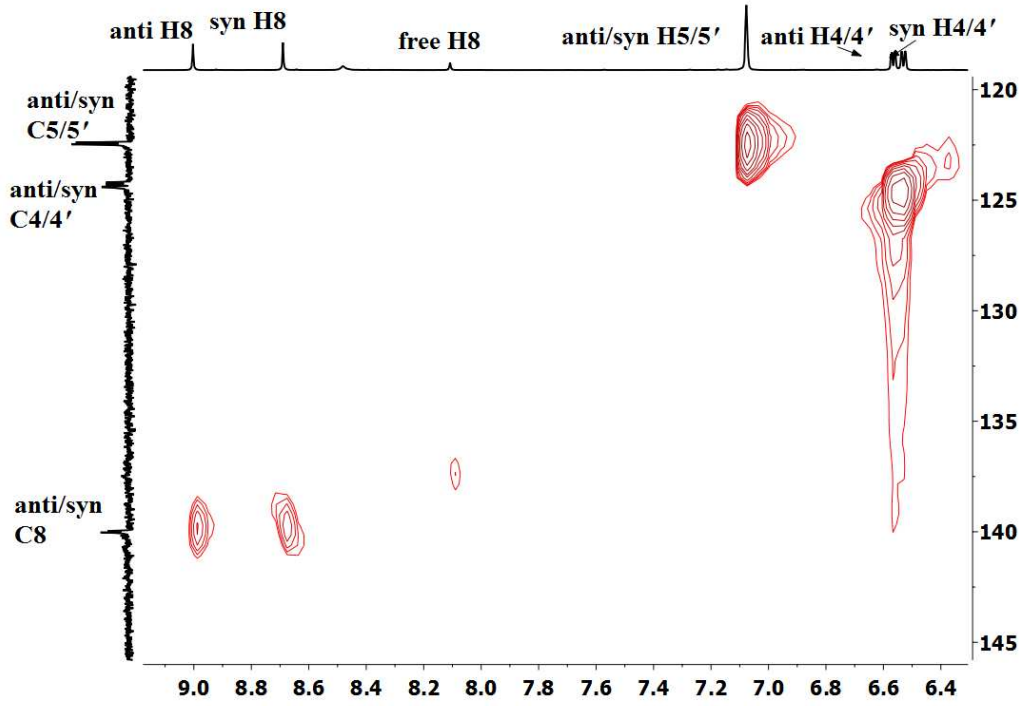

Figure S19. ^{1}H-^{13}C HSQC spectrum (aromatic region) of the Pt(*N*(H)1,1′-Me$_2$dma)(5'-GMP) adduct (25 °C, D_2O, pH 4, shifts in ppm).

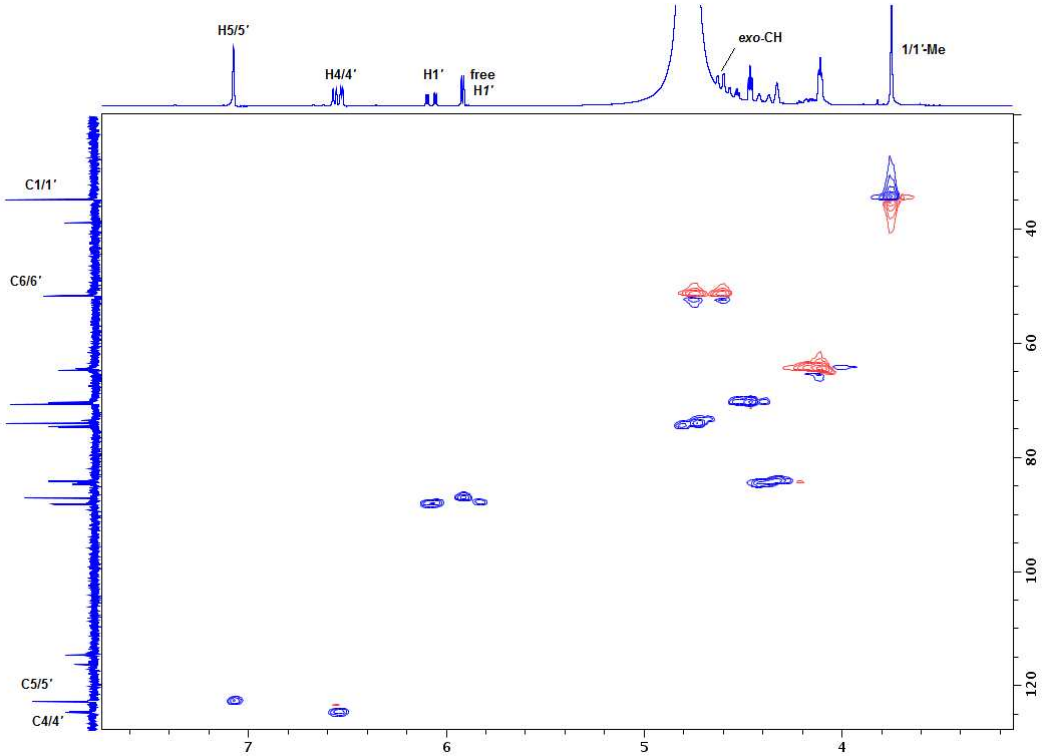

Figure S20. ^{1}H-^{13}C HSQC spectrum (selected region) of the Pt(*N*(H)1,1′-Me$_2$dma)(5'-GMP) adduct (25 °C, D_2O, pH 4, shifts in ppm).

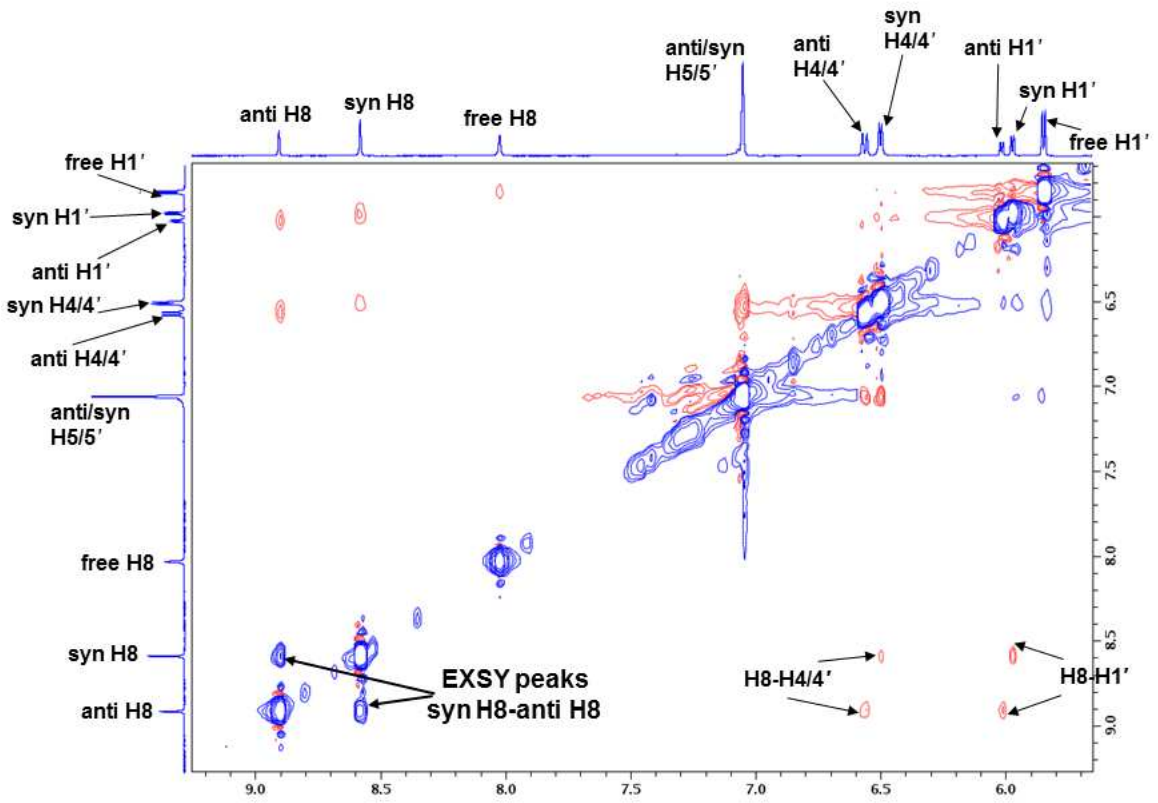

Figure S21. A selected region of the ^{1}H-^{1}H ROESY spectrum of the Pt(*N*(Me)1,1′-Me$_2$dma)(5′-GMP) adduct (25 °C, D$_2$O, pH 4, shifts in ppm).

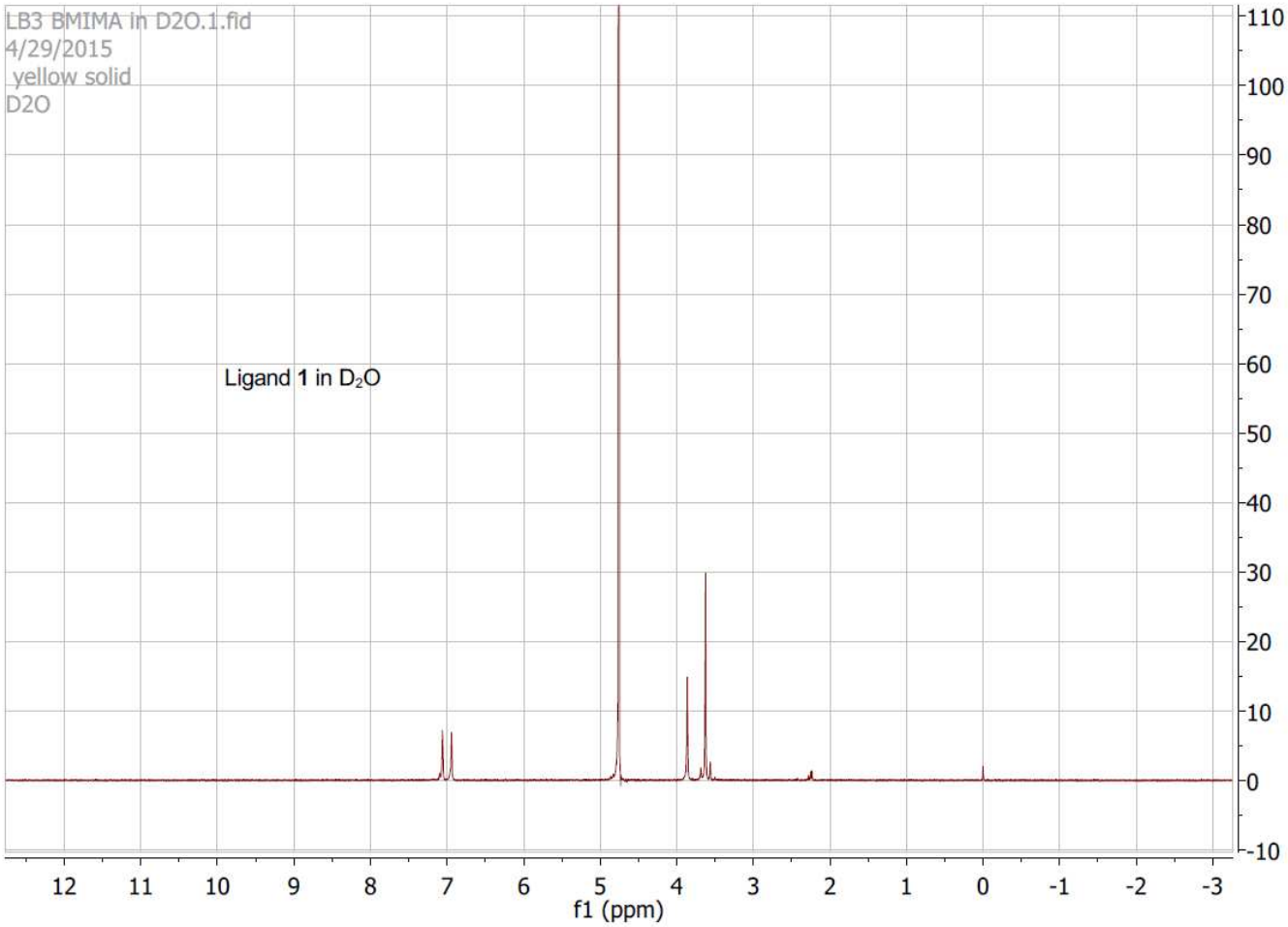

Figure S22. Copy of the ^{1}H NMR spectrum of *N*(H)1,1′-Me$_2$dma (**1**) in D_2O (pH 8.0).

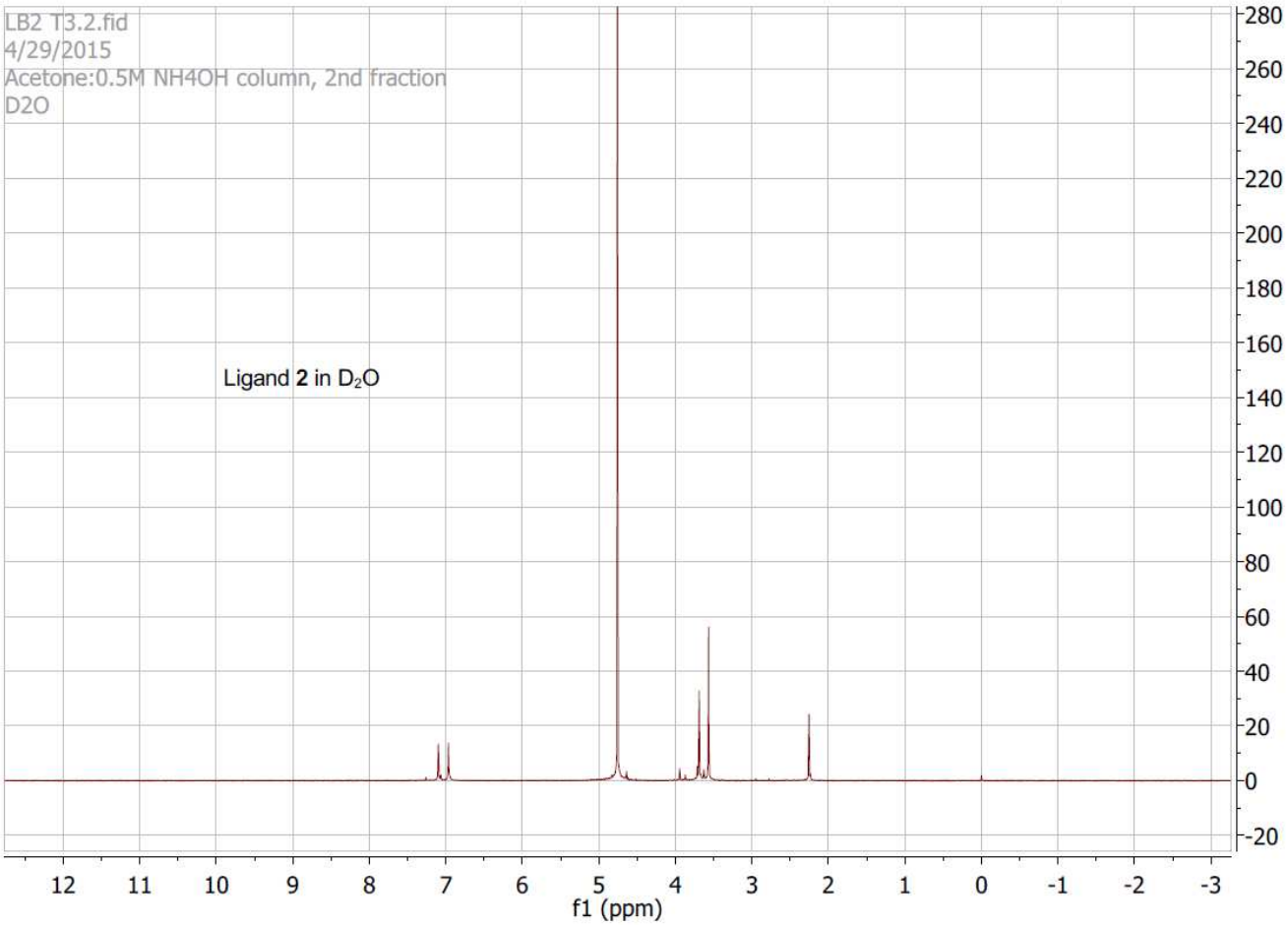

Figure S23. Copy of the ^{1}H NMR spectrum of *N*(Me)1,1′-Me_2dma (**2**) in D_2O (pH 8.3).

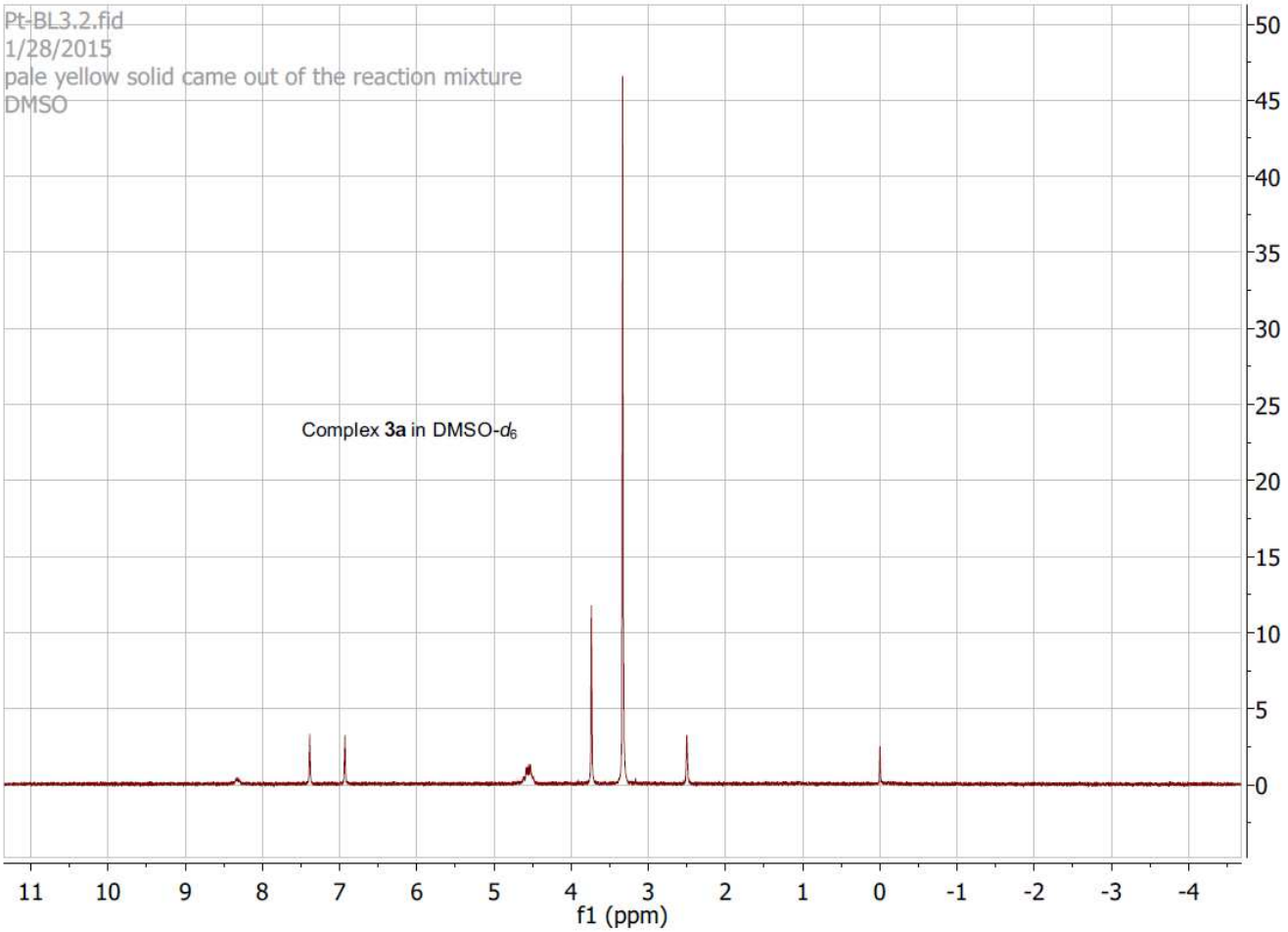

Figure S24. Copy of the ^{1}H NMR spectrum of [Pt(*N*(H)1,1′-Me$_2$dma)Cl]Cl (**3a**) in DMSO-d_6.

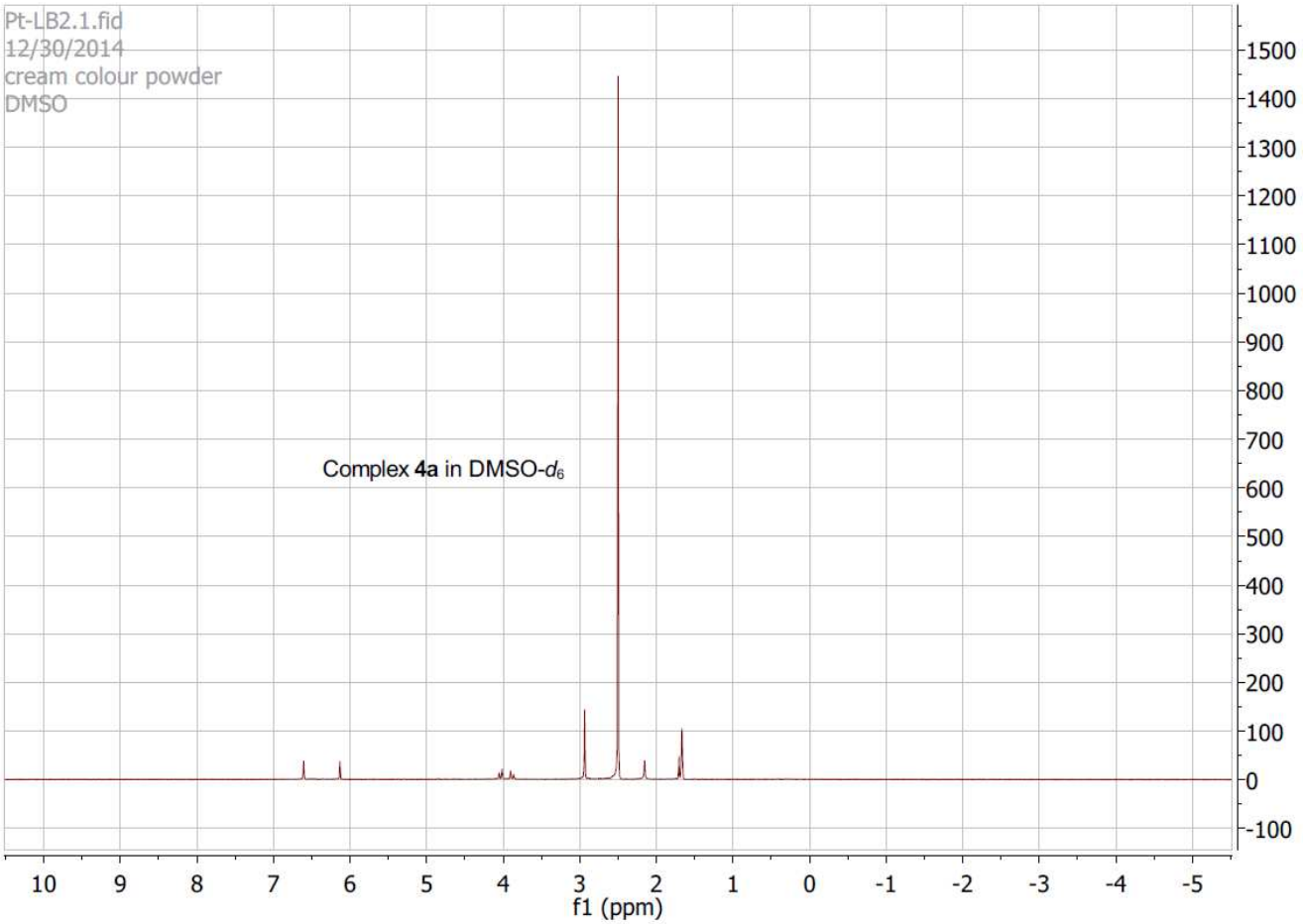

Figure S25. Copy of the ^{1}H NMR spectrum of [Pt(*N*(Me)1,1′-Me_2dma)Cl]Cl (**4a**) in DMSO-d_6.

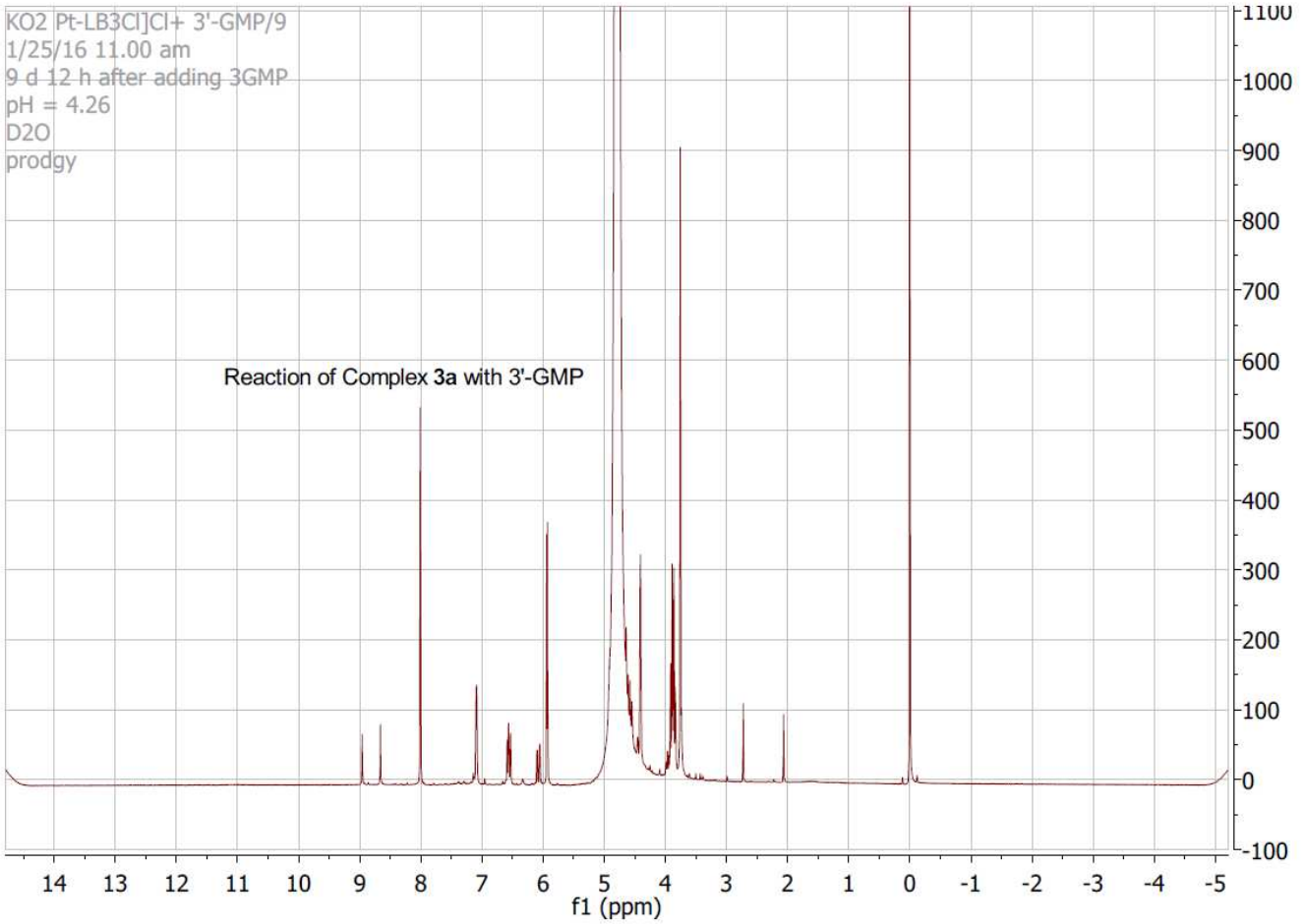

Figure S26. Copy of the final ^{1}H NMR spectrum of the reaction mixture after the formation of the Pt(*N*(H)1,1′-Me_2dma)(3′-GMP) adduct in D_2O.

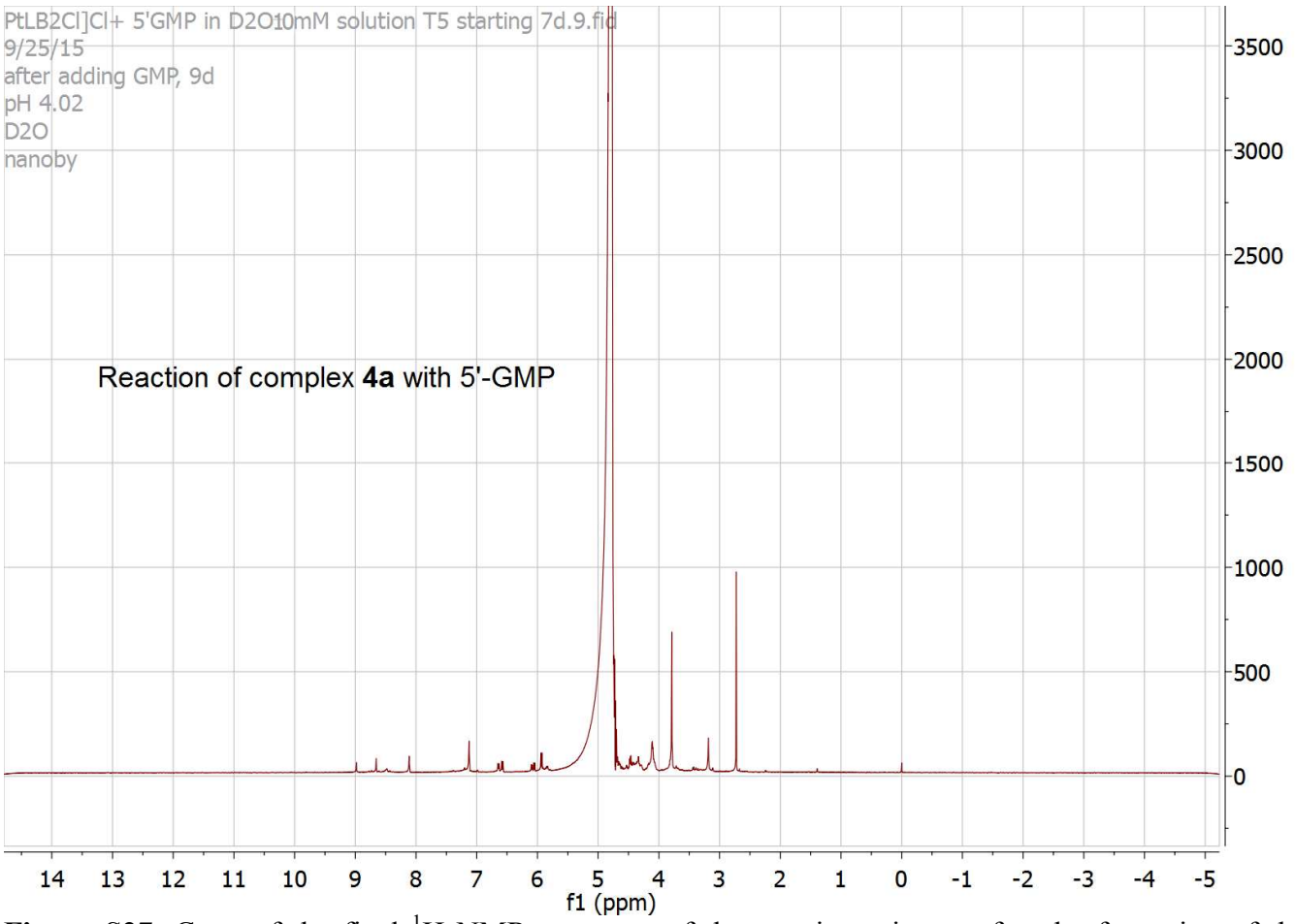

Figure S27. Copy of the final ^{1}H NMR spectrum of the reaction mixture after the formation of the Pt(*N*(Me)1,1′-Me_2dma)(5′-GMP) adduct in D_2O.

Table S1. ^{1}H NMR Shifts (ppm) for the *N*(H)1,1′-Me$_2$dma Carrier Ligands in Pt(*N*(H)1,1′-Me$_2$dma)**G** Adducts and in [Pt(*N*(H)1,1′-Me$_2$dma)Cl]Cl in 65:35 D$_2$O:DMSO-d_6 (pH 4.0) at 25 °C. (Data[11] for [Pt(*N*(H)dpa)(Cl)]Cl and Pt(*N*(H)dpa)**G** Are Included for Comparison.)

Complex	H4/4′ or H6/6′		H5/5′	Me-1/1′	*N*(Me)
	syn	anti			
[Pt(*N*(H)1,1′-Me$_2$dma)Cl]Cl[a]	6.80		7.02	3.56	-
Pt(*N*(H)1,1′-Me$_2$dma)(5′-GMP)[a]	6.41, 6.39	6.44	6.96[b]	3.57	-
Pt(*N*(H)1,1′-Me$_2$dma)(5′-GTP)[a]	6.39, 6.37	6.42	6.97[b]	3.57	-
[Pt(*N*(H)dpa)(Cl)]Cl	8.61		7.34	-	-
Pt(*N*(H)dpa)(5′-GMP)	7.51, 7.44	7.57	7.21	-	-
Pt(*N*(H)dpa)(5′-GTP)	7.49, 7.43	7.57	7.23	-	-

[a] *endo* and *exo*-H6/6′ are masked by the solvent peak. [b] syn and anti signals are overlapped.

Table S2. Selected ^{1}H NMR Shifts (ppm) for **G** in Pt(*N*(H)1,1′-Me$_2$dma)**G** Adducts 65:35 D$_2$O:DMSO-d_6 (pH 4.0) at 25 °C. (Data for Pt(*N*(H)dpa)**G**[11] Are Included for Comparison.)

Complex	H8 free	H8 syn	H8 anti	H1′ free	H1′ syn	H1′ anti	syn:anti ratio	Δδ
Pt(*N*(H)1,1′-Me$_2$dma)(5′-GMP)	7.95	8.57	8.86	5.71	5.85	5.89	1.08:1	0.29
Pt(*N*(H)1,1′-Me$_2$dma)(5′-GTP)	7.98	8.61	8.91	5.71	5.85	5.90	0.95:1	0.30
Pt(*N*(H)dpa)(5′-GMP)	7.96	8.72	9.08	5.71	5.91	5.98	1.14:1	0.36
Pt(*N*(H)dpa)(5′-GTP)	7.97	8.79	9.21	5.70	5.91	5.98	0.82:1	0.42

(1) Benedetti, M.; Tamasi, G.; Cini, R.; Natile, G. X-Ray Structure and Circular Dichroism of Pure Rotamers of Bis[guanosine-5′-monophosphate(−1)](*N,N,N′,N′*-tetramethylcyclohexyl-1,2-diamine)platinum(II) Complexes That Have *R,R* and *S,S* Configurations at the Asymmetric Diamine. *Chem. -Eur. J.* **2003**, *9*, 6122-6132.

(2) Benedetti, M.; Tamasi, G.; Cini, R.; Marzilli, L. G.; Natile, G. The First Pure ΛHT Rotamer of a Complex with a cis-[Metal(nucleotide)$_2$] Unit: A cis-[Pt(amine)$_2$(nucleotide)$_2$] ΛHT Rotamer with Unique Molecular Structural Features. *Chem. -Eur. J.* **2007**, *13*, 3131-3142.

(3) Sheldrick, W. S. Characterisation of a Binary Transition Metal Complex of a Purine 3-Nucleotide, {[Cu_3(3′-GMP)$_2$(3′-GMPH)$_2$(H_2O)$_5$]·7H_2O}$_n$ [1] Phosphate-only Binding of Copper(II). *Z. Naturforsch.* **1983**, *38 b*, 16-19.

(4) Saenger, W. *Principles of Nucleic Acid Structure*; Springer: Berlin, 1984, pp 9-27.

(5) Barnham, K. J.; Bauer, C. J.; Djuran, M. I.; Mazid, M. A.; Rau, T.; Sadler, P. J. Outer-Sphere Macrochelation in [Pd(en)(5′-GMP-*N7*)$_2$]·9H_2O and [Pt(en)(5′-GMP-*N7*)$_2$]·9H_2O: X-Ray Crystallography and NMR Spectroscopy in Solution. *Inorg. Chem.* **1995**, *34*, 2826-2832.

(6) Djuran, M. I.; Milinkovic, S. U.; Habtemariam, A.; Parsons, S.; Sadler, P. J. Crystal packing and hydrogen bonding in platinum(II) nucleotide complexes: X-Ray crystal structure of [Pt(MeSCH_2CH_2SMe)(5′-GMP-*N7*)$_2$]·6H_2O. *J. Inorg. Biochem.* **2002**, *88*, 268-273.

(7) Altona, C.; Sundaralingam, M. Conformational Analysis of the Sugar Ring in Nucleosides and Nucleotides. New Description Using the Concept of Pseudorotation. *J. Am. Chem. Soc.* **1972**, *94*, 8205-8212.

(8) Okamoto, K.; Behnam, V.; Tan Phan Viet, M.; Polissiou, M.; Gauthier, J.-Y.; Hanessian, S.; Theophanides, T. FT-IR and ^{1}H NMR Spectroscopic Studies of C2′- endo, C3′-endo Sugar Ring Conformations in 5′-GMP and 3′-GMP Nucleotides and Their Platinum Complexes. *Inorg. Chim. Acta* **1986**, *123*, L3-L5.

(9) Reily, M. D.; Marzilli, L. G. Novel, Definitive NMR Evidence for N(7), and -PO_4 Chelation of 6-Oxopurine Nucleotide Monophosphates to Platinum Anticancer Drugs *J. Am. Chem. Soc.* **1986**, *108*, 8299-8300.

(10) Melanson, R.; Rochon, F. D. The Molecular and Crystal Structure of (Diethylenetriamine)(inosine)platinum(II) Dinitrate Monohydrate. *Acta Crystallogr., Sect. B: Struct. Sci.* **1978**, *34*, 3594-3598.

(11) Andrepont, C.; Marzilli, P. A.; Marzilli, L. G. Guanine Nucleobase Adducts Formed by [Pt(di-(2-picolyl)amine)Cl]Cl: Evidence That a Tridentate Ligand with Only in-Plane Bulk Can Slow Guanine Base Rotation. *Inorg. Chem.* **2012**, *51*, 11961-11970.